Part 6

Emission and Plasma Theory

Section B. High-Energy Emission

High Energy Radiation from Pulsars

K.S. Cheng

The University of Hong Kong, Pokfulam Road, Hong Kong, China.

Abstract. We propose a three dimensional pulsar magnetosphere model in which the vertical size of the outer gap is first determined by a self-consistent model in which the outer gap is limited by the pair production from collisions of thermal photons produced by polar cap heating of backflow outer gap current and the curvature photons emitted by the gap accelerated charged particles. The transverse size of the outer gap is determined by local pair production condition. In principle, there are two topologically disconnected outer gaps existing in the magnetosphere of a pulsar and both incoming and outgoing particle flows are allowed. And yet double-peak light curves with strong bridges are most common. Using this model and its local properties, we compare the model results with phase-resolved spectra of the Crab pulsar and Geminga.

1. Introduction

It has been argued that powerful acceleration regions, called "outer gaps", can form in the vicinity of "null charge surface" ($\mathbf{\Omega} \cdot \mathbf{B} = 0$) (Holloway 1973; Cheng, Ruderman & Sutherland 1976) because the charged carriers on each side of the null charge surface have opposite charges. Current passing through this surface remove charges in the vicinity of the null surface and a vacuum will form there. Cheng, Ho and Ruderman (1986a,b, hereafter CHR model) used an outer gap model to calculate the phase-averaged spectrum of the Crab pulsar. Their model assumed that the radiation regions are thin in the longitudinal direction. This assumption can be easily justified in the case of the Crab pulsar but certainly cannot be true in Geminga which has a period much longer than that of the Crab pulsar. Zhang and Cheng(1997) have considered a self-consistent thick outergap model in which the pairs are created via collisions between gap curvature photons and soft X-rays from polar cap, which are produced by the backflow outergap current. They use this model to explain efficiencies of X-rays and γ-rays (Cheng, Gil and Zhang 1998; Zhang and Cheng 1998), distributions of basic pulsar parameters, i.e. period, magnetic field, distance and energy flux (Cheng and Zhang 1998, Zhang and Cheng 1999) and phase-average spectra of X-ray and γ-ray pulsars(Cheng and Zhang 1998; Cheng and Zhang 1999).

In these models, the double peak γ-ray structure was from two topologically disconnected outer gaps, each of which is associated with different magnetic poles. However, Romani and his co-workers (Chiang & Romani, 1992,1994; Romani and Yadigaroglu 1995; Romani 1996) have shown that *only one* outer gap with only outgoing current can already produce a double-peak γ-ray light

curve in a three-dimensional outer-magnetosphere. Using a rotating dipolar field plus effects of time travel and aberration, they showed that an assumed outgoing current alone could produce a broad, irregularly-shaped emission beam of which is particularly dense near the edge, so that two γ-ray peaks would be observed when the line of sight from the Earth crosses these enhanced γ-ray beam regions; the inner region of the beam provided a significant amount of emission between the peaks. EGRET has accumulated enough photons for Crab, Vela, PSR B1706-44 and Geminga to analyze the phase-resolved emission characteristics such as pulsed profiles and phase-resolved spectra (Thomson et al. 1996; Fierro et al. 1998). These data can give very strong constraint in theoretical models.

Here, we re-consider the three dimensional magnetosphere, following the important ground-breaking work of Romani and co-workers. But instead of assuming a *single* outer gap with *only* an outgoing current, and no restriction on azimuthal directions, we use various physical processes (including pair production which depends sensitively on the local electric field and the local radius of curvature, surface field structure, reflection of $e^{\pm}$ pairs because of mirroring and resonant scattering) to determine the three-dimensional geometry of the outer gap. In our model, two outer gaps and both outgoing and incoming currents are in principle allowed, but it turns out that outgoing currents dominate the emitted radiation intensities.

2.   Pair Production and the Structure of Outer gaps

We propose a structure of outer gaps determined by pair production conditions. The potential drop of the gap $\Delta V \approx 6.6 \times 10^{12} f_0^2 B_{12} P^{-2}$, where $f_0 = h(< r >)/R_L$, $h(< r >)$ is the average vertical separation of the gap boundaries in the (Ω, μ) plane and $R_L = c/\Omega$ is the light cylinder radius, and $< r >$ is the average distance to the gap; its value depends on magnetic inclination angle χ ($< r > \sim R_L/2$). The particle current passing through the gap is $\dot{N}_{gap} = 3 \times 10^{30} f_0 \xi B_{12} P^{-2}$ s^{-1}, where $\xi = \Delta\Phi/2\pi$; $\Delta\Phi$ is the transverse (ϕ-direction) extension of the gap. Each of the charged particles inside the gap will radiate high-energy curvature photons with a characteristic energy $E_\gamma(f_0) \approx 2 \times 10^8 f_0^{3/2} B_{12}^{3/4} P^{-7/4}$ eV. About half of $\dot{N}_{gap}$ will move toward the star. Although they continue to radiate their energies on the way to the star, they still carry $10.5 P^{1/3}$ ergs of energy on to the stellar surface. The energy will be radiated back out in hard X-rays. However, resonant scattering with pairs near the star may reflect hard X-rays back to the stellar surface (Cheng, Gil & Zhang 1998; Wang et al. 1998), to be re-emitted as soft X-rays with a temperature $T_s \approx 3.8 \times 10^6 f_0^{1/4} \xi^{1/4} B_{12}^{1/2} P^{-5/12}$ K. It is interesting to note that the thermal hard X-rays are reflected back to the stellar surface but there is a non-thermal hard X-rays emitted by the secondary pairs before they form blanket. This non-thermal hard X-ray has been observed (cf. Becker and Trumper 1997) and explained in terms of outergap model(Cheng, Gil and Zhang 1998)

The soft X-ray photon density is very low but each pair produced by an X-ray-curvature photon collisions in the outer gap will emit almost 10^5 curvature γ-rays for further pair creation in that gap. Once the pair production threshold

condition $kT_sE_\gamma \geq (m_ec^2)^2$ is satisfied, the gap is unlikely to grow much larger. This pair production condition gives

$$f_0 = 5.5P^{26/21}B_{12}^{-4/7}\xi^{1/7} \quad . \tag{1}$$

Here, ξ is still an unknown quantity. However, we see that f_0 is weakly dependent on ξ which is likely of order of unity. In first approximation, we assume $f_0 = 5.5P^{26/21}B_{12}^{-4/7}$ (Zhang & Cheng 1997). To determine ξ, we need to consider local pair production processes. The pair production per unit length inside the gap is a decreasing function of r. According to Cheng, Ho and Ruderman (1986), $E_\parallel \propto r^{-1/2}$ for the thin outer gap (e.g. the Crab pulsar), which gives $E_\gamma(r) \propto r^{-1/8}$ after using the large r limit $s(r) = (rR_L)^{1/2}$. Since E_γ is only weakly dependent on r, we assume $\sigma_{\gamma\gamma} \approx const$. The local pair production per unit length is $N_{e\pm}(r) = (1 - e^{-\tau_{\gamma\gamma}})N_\gamma(r) \approx \tau_{\gamma\gamma}N_\gamma(r)$, where $\tau_{\gamma\gamma} = n_X(r)\sigma_{\gamma\gamma}l(r)$ is the local optical depth, $n_X = R^2T_s^4\sigma/r^2kT_sc$ is the X-ray number density at r, $l(r) \approx (2s(r)f(r)R_L)^{1/2}$ is the local optical path, $f(r) = h(r)/R_L$ is the local vertical extension of the gap (since $B(r)h^2(r)$ is a constant, which gives $f(r) \propto r^{3/2}$ and $f_0 \sim f(R_L/2)$), and $N_\gamma = eE_\parallel(r)/E_\gamma(r)$ is the number of curvature photons emitted at r per e^+/e^- per unit length, then $N_{e\pm}(r) \propto r^{-11/8}$. We see that most pairs are produced near the null surface where $r = r_{in}$. We estimate that the pair production will take place mainly in the range $r_{in} \leq r \leq r_{lim}$ where r_{lim} is estimated as $r_{lim}N_{e\pm}(r_{lim})/r_{in}N_{e\pm}(r_{in}) \sim (r_{lim}/r_{in})^{-3/8} \sim 1/2$, which gives $r_{lim} \sim 6r_{in}$. This limits pair production both along the field lines and in transverse directions, and gives $\Delta\Phi \sim 160°$. Within the pair production regions, outgoing and incoming directions for particle flows are allowed. For $r > r_{lim}$ only outgoing current is possible. For thick outergap, we (Zhang and Cheng 1999) have argued that the radial extension of the thick outergap must be $r_{lim} \approx f_oR_L$. For the parameters of Geminga pulsar, this gives $\Delta\Phi \sim 150°$.

3. Photon Emission Morphologies

In order to show the high energy photon morpholgy emitted from outer gaps, we need a polar cap shape for a given magnetic inclination. Polar cap shape defines the boundary of the open volume at the stellar surface. Because the outer gap is within the open volume, we divide the open volume into many parts, in which the shape of each part at the stellar surface is the same as the polar cap shape but the size is smaller. First we determine the coordinate values (x_0, y_0, z_0) of the last closed field lines at the stellar surface. Then the coordinate values (x_0', y_0', z_0') for different parts can be determined by using $x_0' = a_1x_0$, $y_0' = a_1y_0$ and $z_0' = (1 - (x_0'^2 + y_0'^2))^{1/2}$ and by changing a_1. Once the polar cap shape is defined, we find the last closed field lines using Runge-Kutta integration: (i) give a set of initial values at the stellar surface; (ii) use the Runge-Kutta integration to follow a particular field line in space and determine whether this line closes inside the light cylinder or crosses it and (iii) iterate on the initial value until the field line is just tangential to the light cylinder. Furthermore, we assume that relativistic charged particles in the open zone radiate in their direction of propagation, i.e. along the magnetic field lines in the corotating frame. For each location within
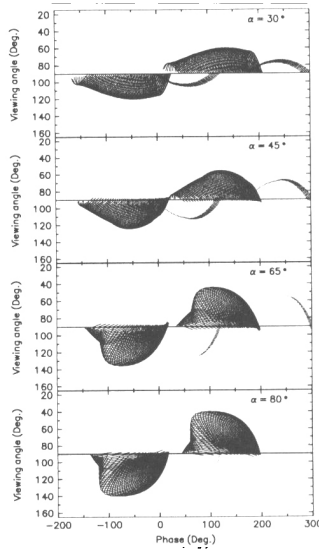
Figure 1.   The emission morphologies for various inclination angle α. The parameters of the Crab pulsar are used.

the open zone the direction of emission expressed as (ζ, Φ) is calculated, where ζ is the polar angle from the rotation axis and Φ is the phase of rotation of the star. In these calculations, the effects of travel time and aberration are taken into account. A photon with velocity $\mathbf{u} = (u_x, u_y, u_z)$ along a magnetic field line with a relativistic addition of velocity along the azimuthal angle gives an aberrated emission direction $\mathbf{u}' = (u'_x, u'_y, u'_z)$. Travel time gives a change of the phase of the rotation of the star. Combining these two effects, and choosing $\Phi = 0$ for radiation in the (x, z) plane from the center of the star, ζ and Φ are given by (Yadigaroglu, 1997 Ph.D.thesis, Stanford University)

$$\cos \zeta = u'_z \qquad (2)$$
$$\Phi = -\phi_{u'} - \vec{r} \cdot \hat{u}' ,$$

where $\phi_{u'}$ is the azimuthal angle of $\hat{u}'$ and $\vec{r}$ is the emitting location in units of R_L. We project photon emissions on the (ζ, Φ) plane and observe the emission patterns on the sky. In (ζ, Φ) plane, the null surface can be determined easily because it consists of the points at which magnetic field lines are perpendicular to the rotation axis. For a field line, the null charge crossing is the location which the projected line crosses the equatorial line ($\zeta = 90°$). Fig. 1 shows emission morphologies for various inclination angle α. The observed light curve can be obtained by given ζ and α.

4.   Phase-resolved spectra of Crab and Geminga Pulsars

From the emission morphologies we see that photons emitted into a given phase come from different positions of the outergap. Since curvature radiation, synchrotron radiation and inverse Compton scattering depend on local quantities,
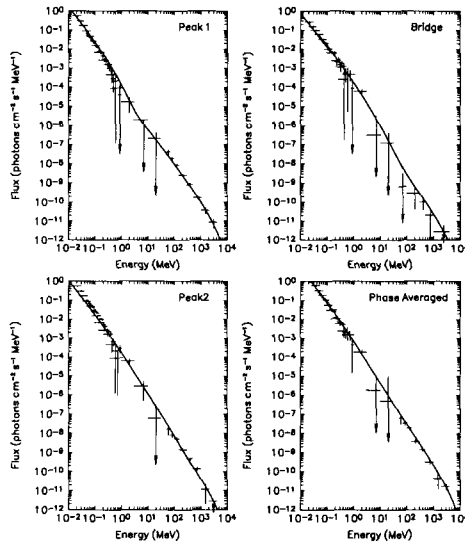
Figure 2. Phase-resolved γ-ray spectra from 10MeV to 10GeV for peak 1, bridge, peak 2 and phase-average of the Crab pulsar. Observed data are taken from Ulmer et al. (1995).

e.g. curvature, $E_{\parallel}$, B, n_{ph} etc., it is likely that the radiation spectrum varies with phase. Fig.2 shows the comparison of model calculated spectra and observed phase-resolved data of the Crab pulsar. Fig.3 shows the comparison of model calculated spectra and observed phase-resolved data of the Geminga pulsar.

5. Summary and Discussion

We use a 3-D model magnetospheric model to calculate the emission morphologies and the phase-resolved spectra of the γ-ray pulsars. In our model, the local photon-photon pair production in the outer gaps limits the extension of the outer gaps along the azimuthal direction. We find that the two topological disconnected outer gaps, with some extension along the azimuthal (ϕ) direction, exist in the pulsar magnetosphere. Double-peaked pulse profiles with varying phase separation, depending on viewing angle, and strong bridge emission occur naturally, as in the single pole outer gap model. Our model successfully explain the observed phase-resolved spectra from the Crab pulsar and the Geminga pulsar in peak one, trailing wing one, bridge, leading wing two, peak 2 and phase-average. However, our model cannot produce the off-pulse radiation, perhaps they come from particles with larger pitch angles and/or tertiary pairs which we have ignored in our calculation. Finally, we want to remark that our calcualtion is based on the steady state accelerator. The realistic outermagnetospheric gap may be a dynamical or flickering one.
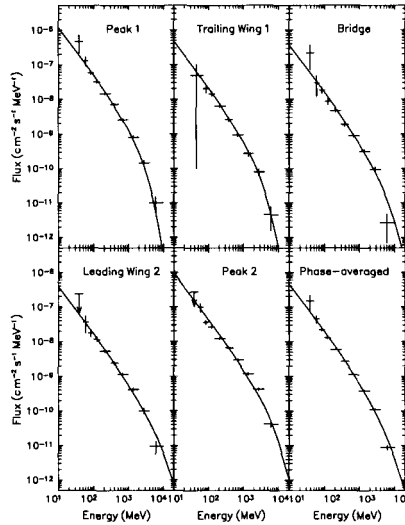
Figure 3.   Phase-resolved γ-ray spectra for different phases (peak one, trailing wing one, bridge, leading wing two, peak 2 and phase-average) of the Geminga pulsar. Observed data are taken from Fierro et al. (1998).

References

Becker, W. & Trumper, J., 1997, A&A, 326, 682

Cheng, A.F., Ruderman, M.A. & Sutherland, P.G., 1976, ApJ, 203, 209

Cheng, K.S., Ho, C. & Ruderman, M.A., 1986a, ApJ, 300, 500 (CHR I)

Cheng, K.S., Ho, C. & Ruderman, M.A., 1986b, ApJ, 300, 522 (CHR II)

Cheng, K.S., Gil, J & Zhang, L., 1998, ApJ, 493, L35

Cheng, K.S. & Zhang, L., 1998, ApJ, 498, 327

Cheng, K.S. & Zhang, L., 1999, ApJ, 515, 337

Chiang, J. & Romani, R.W., 1992, ApJ, 400, 724

Chiang, J. & Romani, R.W., 1994, ApJ, 436, 754

Fierro, J.M., Michelson, M., Nolan, P.L. & Thomson, D.J., 1998, ApJ, 494, 734

Holloway, N.J., 1973, Nature Physical Science, 246, 6

Romani, R.W., 1996, ApJ, 470, 469

Romani, R.W. & Yadigaroglu, I.-A., 1995, ApJ, 438, 314

Thompson , D.J. et al., 1996, ApJ, 465, 385

Ulmer, M.P. et al., 1995, ApJ, 448, 356

Wang, F.Y.-H., Ruderman, M., Halpern, J.P. & Zhu, T., 1998, ApJ, 498, 373

Zhang, L. & Cheng, K.S., 1997, ApJ, 487, 370